Dendrochronologia 78 (2023) 126057

Contents lists available at ScienceDirect

Dendrochronologia

journal homepage: www.elsevier.com/locate/dendro

Seasonal precipitation and continentality drive bimodal growth in Mediterranean forests

Cristina Valeriano [a,b], Emilia Gutiérrez [c], Michele Colangelo [a], Antonio Gazol [a], Raúl Sánchez-Salguero [d], Jan Tumajer [e], Vladimir Shishov [f], José Antonio Bonet [g,h], Juan Martínez de Aragón [h], Ricardo Ibáñez [i], Mercedes Valerio [i], J. Julio Camarero [a,*]

[a] Instituto Pirenaico de Ecología (IPE-CSIC), Avda. Montañana 1005, Zaragoza E-50192, Spain
[b] Department of Natural Systems and Resources, Universidad Politécnica de Madrid, Madrid, Spain
[c] Department of Biological Evolution, Ecology and Environmental Sciences, Faculty of Biology, Universitat de Barcelona, Barcelona, Spain
[d] Departamento de Sistemas Físicos, Químicos y Naturales, Universidad Pablo de Olavide, Sevilla 41013, Spain
[e] Department of Physical Geography and Geoecology, Faculty of Science, Charles University, Albertov 6, Prague 12843, Czech Republic
[f] Mathematical Methods and IT Department, Siberian Federal University, Krasnoyarsk, Russia
[g] Department of Crop and Forest Sciences, University of Lleida, Av. Alcalde Rovira Roure 191, Lleida E-25198, Spain
[h] Joint Research Unit CTFC, AGROTECNIO, CERCA, Ctra. Sant Llorenç de Morunys km 2, Solsona 25280, Spain
[i] Departamento de Biología Ambiental, Facultad de Ciencias, Universidad de Navarra, Calle Irunlarrea 1, Pamplona 31008, Spain

ARTICLE INFO

Keywords:
Juniperus
Vaganov-Shashkin model
Phenology
Pinus
Radial growth
Xylogenesis

ABSTRACT

Tree phenology is sensitive to climate warming and changes in seasonal precipitation. Long xylogenesis records are scarce, thus limiting our ability to analyse how radial growth responds to climate variability. Alternatively, process-based growth models can be used to simulate intra-annual growth dynamics and to better understand why growth bimodality varies along temperature and precipitation gradients. We used the Vaganov-Shashkin (VS) growth model to analyse the main climatic drivers of growth bimodality in eight trees and shrubs conifers (four pines and four junipers) across Spain. We selected eleven sites with different continentality degree and spring/autumn precipitation ratios since we expected to find pronounced bimodal growth in less continental sites with spring and autumn precipitation peaks. The VS model successfully simulated annual growth rates at all sites as a function of daily temperature and soil moisture data. Bimodal growth patterns clustered into less continental sites showing low spring/autumn precipitation ratios. This finding agrees with observed climate-growth associations showing that growth was enhanced by wet-cool winter-to-spring conditions, but also by wet autumn conditions in the most bimodal sites. We observed a stronger growth bimodality in pines compared to junipers. We discuss the spatial variability of climate drivers in bimodality growth pattern and how increasing continentality and shifts in seasonal precipitation could affect growth patterns. Bimodality could be an advantageous response to overcome summer drought in Mediterranean forests. The ability of some species to reactivate growth during autumn might determine their capacity to withstand increasing summer aridity.

1. Introduction

Trees are responding to climate warming through phenological changes due to the increase of temperatures in spring and autumn (Menzel et al., 2006) and the variability of precipitation (Pendergrass et al., 2017). Phenological shifts linked to climate warming have been mainly recorded in temperate and boreal forests, but this pattern is not always observed in seasonally dry Mediterranean forests where phenology depends on precipitation seasonality (Peñuelas et al., 2004). In drought-prone regions of the Mediterranean Basin such as Spain, advanced spring phenology was reported as climate warmed from the 1980 s to the 2000 s, but this was not the case for wet periods such as the

* Corresponding author.
E-mail addresses: cvaleriano@ipe.csic.es (C. Valeriano), emgutierrez@ub.edu (E. Gutiérrez), mcolangelo@ipe.csic.es (M. Colangelo), agazol@ipe.csic.es (A. Gazol), rsanchez@upo.es (R. Sánchez-Salguero), tumajerj@natur.cuni.cz (J. Tumajer), vlad.shishov@gmail.com (V. Shishov), jantonio.bonet@udl.cat (J.A. Bonet), mtzda@ctfc.cat (J. Martínez de Aragón), ribanez@unav.es (R. Ibáñez), mvalerio.1@alumni.unav.es (M. Valerio), jjcamarero@ipe.csic.es (J.J. Camarero).

https://doi.org/10.1016/j.dendro.2023.126057
Received 21 July 2022; Received in revised form 9 January 2023; Accepted 9 January 2023
Available online 11 January 2023

1970 s (Gordo and Sanz, 2005, 2009). Therefore, it is unclear how changes in seasonal precipitation variability and soil water availability will affect tree phenology and growth in seasonally dry Mediterranean areas, given the complex couplings among them (Delpierre et al., 2019; Peñuelas et al., 2002, 2004).

In seasonally dry Mediterranean regions, tree growth is driven, among other factors, by favorable warm and wet climate conditions during spring and autumn (Mitrakos, 1980). These two seasons are characterized by higher radial growth rates than the cold winter and the dry summer leading to bimodal growth patterns with a major growth peak in spring and a secondary peak in autumn (Battipaglia et al., 2016; Camarero et al., 2010; Campelo et al., 2018; Cherubini et al., 2003). Bimodality may be a facultative pattern that changes as a function of site climate conditions (e.g., continentality), species-specific wood phenology (xylogenesis) or year-to-year shifts in seasonal precipitation (Pacheco et al., 2016; Tumajer et al., 2021b). Therefore, a bimodal growth pattern implies that the dynamics of radial growth has a very high responsiveness to climate, a fact more frequently observed in isohydric species showing great plasticity to adjust the dynamics of their radial growth to climatic conditions such as *Pinus halepensis* Mill. (Liphschitz, 1984; De Luis et al., 2011). Bimodal growth in seasonally dry locations or on sites with soils with lower capacity of water retention may be an adaptive mechanism to withstand drought (Del Río et al., 2014; Valeriano, 2017), but this idea has not been tested. These populations show low resistance to extreme droughts but recover more quickly than populations in wet sites (Gazol et al., 2017). Bimodal growth patterns have often been observed in Mediterranean pine species, with a high variability of bimodality intensity across spatial and climatic gradients (Battipaglia et al., 2010; Campelo et al., 2021; De Luis et al., 2007; Pacheco et al., 2016; Vieira et al., 2013).

However, growth bimodality is not exclusive of trees and some species of shrubs can also show this growth pattern (Tumajer et al., 2021b, 2021c) depending on traits including climate sensitivity and water use efficiency (Quero et al., 2011). Interestingly, shrubs play an important role in maintaining the ecological balance of dry Mediterranean ecosystems because they can inhabit stressful sites in which trees are not able to survive (Gazol and Camarero, 2012; Génova et al., 2013; Sánchez-Salguero and Camarero, 2020). Therefore, studies on bimodality in trees and shrubs are needed to disentangle their different intra-annual responsiveness to climate.

Overall, we still lack enough understanding of the climatic triggers of bimodality. Bi- to multi-modal growth patterns have been observed in sites or species showing several precipitation peaks under mild winter conditions (De Luis et al., 2007), or in subtropical pine species (Liu et al., 2018). The fact that bimodality has been observed in monsoon regions with wet summer conditions (Morino et al., 2021; Pompa-García et al., 2021; Zhang et al., 2017) suggests that the bimodal pattern may represent widespread phenological adjustments of the xylem which allow extending the growing season after summer quiescence. In this respect, Oberhuber et al. (2021) induced bimodality in *P*inus *sylvestris* L. by blocking phloem transport thus shifting carbon availably. However, it has been also observed that bimodality may be facultative and only occur if there are enough precipitation in both spring and autumn and mild temperatures (Campelo et al., 2021). Tracking the occurrence of bimodal growth patterns across species and continentality gradients is fundamental to advance in the understanding of the bimodal growth pattern of Mediterranean trees and shrubs.

Mediterranean forests and shrublands are sensitive to precipitation shortage through the reduction of soil moisture availability. This can lead to reduced growth rates in spring or autumn, extension of cambial quiescence during the dry summer or shortening the growing season. Since the impacts of drier and warmer conditions can differently affect growth rates and growth duration (Cuny, 2015; Lempereur et al., 2015), we need more information on the timing and rates of spring and autumn growth of Mediterranean trees and shrubs. This is hampered by the lack of long xylogenesis records, which are needed to assess seasonal couplings between climate and intra-annual growth under climate change (see Delpierre et al., 2019). Alternatively, process-based models such as the Vaganov—Shashkin model (VS model) can be used to simulate intra-annual radial growth dynamics (Vaganov et al., 2006). The VS model simulates annual growth rates (ring-width indices) from climatic input variables, and it has allowed to assess climate-change effects on simulated growth phenology (He et al., 2018; Tumajer et al., 2021a; Yang et al., 2017). In the Mediterranean region and other drought-prone areas, the VS model was already shown to produce reliable growth simulations in pine and juniper species (Touchan et al., 2012; Tumajer et al., 2021b; Valeriano et al., 2021b).

Here we used the VS model to detect the main climate drivers of bimodality for eight conifers: five tree species (*Juniperus thurifera* L., *Pinus halepensis*, *Pinus sylvestris*, *Pinus pinaster* Ait. and *Pinus pinea* L.) and three shrub species (*Juniperus communis* L., *Juniperus oxycedrus* L. and *Juniperus phoenicea* L.) inhabiting Mediterranean sites in Spain subjected to different climate continentality and seasonal precipitation regimes. For each species, we selected two sites with contrasting climatic continentality and spring and autumn precipitations. Our specific aims were: (i) to test the ability of the VS model to reproduce growth indices as a function of climate variability, (ii) to assess climate-growth relationships for each species across sites, and (iii) to evaluate the climatic drivers of bimodal growth. We expect to find the most marked bimodal growth patterns in coastal sites with pronounced autumn and spring precipitation peaks.

2. Materials and methods

2.1. Sampled sites and species

We selected eight stands dominated by shade-intolerant conifers (four pines and four junipers) in eleven sites located in Spain (Fig. S1) showing contrasting continentality and spring/autumn precipitation ratios (see climate conditions in Table 1 and Fig. S2). In the Iberian Peninsula, continentality increases towards inland regions, whereas autumn precipitation becomes more important as we approach the Mediterranean coast due to convective storms (Andrade and Corte-Real, 2015; Martín-Vide and Olcina, 2001). Lack of summer precipitation was common to all study sites except Napal, where the summer drought occurred due to southern slope aspect and shallow soils (edaphic drought). By contrast, the summer drought was the most intense in the southernmost Doñana site (Fig. S2).

The two *P. halepensis* sites were located in north-eastern Spain, one near the Mediterranean coast (Garraf) with a mild climate and wet autumns, and the other in the inland, semi-arid and continental middle Ebro Basin with a spring rainfall peak (Peñaflor). The Garraf site has basic soils and it is dominated by *P. halepensis* with other Mediterranean species such as *Quercus ilex* L. (Campelo et al., 2018, 2021; Gazol et al., 2017). In Peñaflor, *P. halepensis* coexists with shrubs (*J. phoenicea*) and tree species (*J. thurifera*) under Mediterranean continental conditions. In this site, soils are formed by gypsum and marls and the summer drought may last 3–4 months (Camarero et al., 2015, 2021a). Here, drought-induced dieback of *P. halepensis* has been observed (Camarero et al., 2015; Valeriano et al., 2021a).

In the case of *P. sylvestris* and *P. pinaster*, we selected two sites where both species coexisted. One site is located near the Mediterranean coast, in the Prades mountains (north-eastern Spain), and the other (Valonsandero) is situated inland, near Soria city (north-central Spain), and subjected to continental conditions with cold winters and a short growing season. In both sites, sampled trees were planted and have similar age, soils were acid. In Prades, natural vegetation consists of *Q. ilex*, *Arbutus unedo* L. and *Phillyrea latifolia* L. in the understory (Collado et al., 2019).

The two *P. pinea* sites were sampled in the Mediterranean coast (Maresme site, north-eastern Spain) and inland (Viloria site, central Spain) with a continental climate. In both sites, soils were acid and of

Table 1
Characteristics of the study sites. The latitude and longitude in decimal degrees and the elevation in meters above the sea level were measured in situ with a GPS. Climate data (mean annual temperature and annual precipitation) correspond to the 1970–2020 period. JCI is the Johansson Continentality Index and its trend during the period 1970–2019 (italics show non-significant trends, $p > 0.05$). The last column shows means ± standard deviations for the period 1970–2020.

Species (code)	Site (code)	Latitude N	Longitude –W / +E	Elevation (m a.s.l.)	Mean annual temperature (ºC)	Annual precipitation (mm)	JCI	Trend JCI	Spring/autumn precipitation ratio
Pinus sylvestris (Ps) & *Pinus pinaster* (Pp)	Prades (PR)	41.35	1.04	900	15.5	547	32.97	0.132	1.08 ± 0.72
	Valonsadero (VA)	41.78	-2.52	1100	11.2	556	28.32	*0.097*	1.54 ± 1.11
Pinus halepensis (Ph)	Garraf (GA)	41.25	1.90	300	15.7	585	23.98	0.099	0.95 ± 0.64
	Peñaflor (PE)	41.72	-0.78	375	14.5	476	31.12	0.137	1.49 ± 1.05
Pinus pinea (Pi)	Maresme (MA)	41.61	2.62	270	15.2	675	22.06	0.113	0.97 ± 0.65
	Viloria (VI)	41.43	-5.12	775	12.5	432	31.59	*0.098*	1.31 ± 1.24
Juniperus communis (Jc)	Napal (NA)	42.73	-1.23	780	11.2	877	27.68	0.124	1.29 ± 0.76
	Aliaga (AL)	40.67	-0.77	1220	10.1	553	31.54	0.147	1.42 ± 0.97
Juniperus oxycedrus (Jo)	Napal (NA)	42.73	-1.23	780	11.2	877	27.68	0.124	1.29 ± 0.76
	Agüero (AG)	42.31	-0.81	694	12.2	683	30.44	*0.089*	1.27 ± 0.95
Juniperus thurifera (Jt)	Peñaflor (PE)	41.72	-0.78	375	14.6	315	31.12	0.137	1.49 ± 1.05
	Corbalán (CO)	40.43	-0.98	1350	10.1	553	31.55	0.144	1.42 ± 0.97
Juniperus phoenicea (Jp)	Peñaflor (PE)	41.72	-0.78	375	14.6	315	31.12	0.137	1.49 ± 1.05
	Doñana (DO)	37.02	-6.50	14	18.3	534	25.72	0.113	1.12 ± 0.91

sandy texture. In the Maresme site, recent drought-induced dieback was observed after the severe 2015 drought (JJ Camarero, pers. observ.).

We sampled *J. communis* in two relatively continental sites, a wetter site (Napal) and a drier site (Aliaga), since this species is only found in areas with continental influence (Pellizzari et al., 2017; Tumajer et al., 2021b). In both sites, soils are basic and with sandstone texture, and *J. communis* coexists with *J. oxycedrus*.

We selected Napal and the drier and warmer Agüero site for sampling *J. oxycedrus* (Fig. S2). In Agüero, soils are basic and develop on clays and sandstone. Then, *J. thurifera* was sampled in the dry Peñaflor site, where it coexists with *P. halepensis* and *J. phoenicea* (Camarero et al., 2021b), and in the continental Corbalán site where soils are loamy and basic (Camarero et al., 2015). Since *J. thurifera* is found in sites under continental influence from southern France to north-western Africa, it was not possible sampling sites with a low continentality degree.

Lastly, we sampled *J. phoenicea* in a coastal site (Doñana, south-western Spain) and in a continental site (Peñaflor), already described for *P. halepensis*. In Doñana, junipers were sampled on sandy soils, in dunes, after a drought-induced dieback episode starting in 2005 (Camarero et al., 2020).

2.2. Climate data

Daily, monthly and seasonal series of climate data (mean temperature, total annual precipitation) for the common 1970–2020 period were obtained from the 0.25º-gridded E-OBS climate dataset (Cornes et al., 2018). Monthly temperature and precipitation series were converted into seasonal temperature means and precipitation totals, respectively. Seasons were defined as follows: winter, previous December to current February; spring, March to May; summer, June to August; and autumn, September to November. Next, we calculated the ratio between spring and autumn precipitation (below the threshold of 1, the autumn rainfall is higher than spring and vice versa) to assess how precipitation varies between the two seasons with the highest growth rates in Mediterranean forests (Mitrakos, 1980; Camarero et al., 2010). The Johansson Continentality Index (JCI, Eq. 1) was used to evaluate the continentality degree of sampling sites since it was shown to adequately characterize continentality gradients across Spain (Andrade and Corte-Real, 2015).

$$JCI = (1{\cdot}7 \times Tamp / \sin \varphi) - 20{\cdot}4 \quad (1)$$

where Tamp is the annual range of the monthly mean air temperatures (ºC) and sin φ is the sine of the geographical latitude (φ). This index was calculated for the period 1970–2019. An oceanic or maritime climate is considered if JCI < 33, whereas continental climates correspond to JCI > 34 (Andrade and Corte-Real, 2015).

2.3. Tree-ring width data

We selected from 14 to 42 dominant and healthy individuals for each species at each site. Sampling was done in 2016–2020. In the case of trees, two cores separated by 180º were extracted at 1.3 m using Pressler increment borers (Haglöf Sweden AB) whereas a basal cross-section of the main stem was taken from shrubs. Cores and shrub sections were air dried and carefully sanded following dendrochronological procedures until ring boundaries were clearly visible (Fritts, 1976). Then samples were scanned at 2400 dpi using a high-resolution scanner (Epson Expression 10.000 XL, Seiko Epson Corp., Japan). Two radii per individual were visually cross-dated and measured. Ring widths were measured with a 0.001 mm resolution using the CDendro and CooRecorder software (Larsson and Larsson, 2018). The quality of the visual cross-dating was checked using the COFECHA software (Holmes, 1983). Tree age was estimated by counting the number of rings in cores and cross-sections from pith to bark.

Each individual ring-width series was detrended by fitting cubic splines with a 0.5 response cut-off at windows of 2/3 length of each series to remove long-term trends in growth due to changes in plant size or disturbances (Cook and Kairiukstis, 1990). Then, ring-width indices were obtained by dividing observed by fitted values. These indices were subjected to autoregressive modelling to remove temporal autocorrelation and to produce residual indices. Lastly, the series of these indices were averaged for each site and species into chronologies using robust bi-weight means. Detrending was done using the dplR package (Bunn, 2010, 2021) in the R statistical software (R Core Team, 2022).

To characterize and compare the site ring-width series or indexed chronologies, we calculated several statistics including the mean and standard deviation of ring widths, the first-order autocorrelation (AR1) of ring widths, which measures year-to-year growth persistence, the mean sensitivity (MSx) of ring-width indices which is a relative measure of width-index changes between consecutives rings, and the mean correlation between indexed ring-width series (rbar) (Fritts, 1976). We also calculated the Expressed Population Signal (EPS) of ring-width chronologies to assess internal replication and coherence as compared with an infinitely replicated chronology (Wigley et al., 1984).

2.4. Climate-growth relationships

To assess how climate drove year-to-year growth variability, we calculated for each species the Pearson correlation coefficients between the residual chronologies of ring-width indices and monthly and

seasonal climate data (temperature and precipitation) considering the common period 1970–2016. Significance and 95–99% intervals for each correlation coefficient were also assessed. These correlations were calculated from previous September to current November, thus covering the period from prior to current autumn.

2.5. Simulations of intra-annual growth dynamics using the VS model

To simulate the intra-annual growth patterns of each species and site, the process-based VS model was calibrated and validated by comparing observed residual ring-width series with simulated series (Vaganov et al., 2006). The latest version of the VS model implemented in the so-called VS-oscilloscope was used (version 1.37, Shishov et al., 2016, 2021). The VS model simulates daily integral growth rates (Gr) reflecting daily temperature, precipitation and day length (outputs GrW, GrT and DOY). The model defines annual simulated growth chronology as standardized sum of Gr during specific year, that is verified against observed site chronology. The model focuses on cambial activity and assumes that daily growth might be limited by low soil water availability (GrW) or low temperature (GrT). Daily soil moisture is estimated based on temperature and precipitation data using an empirical hydrological model (Thornthwaite and Mather, 1955).

The model was calibrated using 16 parameters obtained from previous studies and different sites (see Valeriano et al., 2021b and parameters' description in Table S1). The model was used to simulate chronologies during 1970–2016/2020. We divided the simulation period into calibration (1970–1995) and verification (1996–2016/2020) subperiods, except for *J. communis* and *J. oxycedrus* series with shorter span in which case the periods were 1985–2000 for calibration and 2001–2016 for verification. We calculated several statistics to compare observed and simulated ring-width series (Tychkov et al., 2019). Along with Pearson correlation we obtained the synchronicity index (Gleichläufigkeit statistic, Glk) which measures the percentage of common signs of year-to-year growth change between the two series (Buras and Wilmking, 2015). Next, we obtained the root mean square error (RMSE), a quadratic scoring rule measuring the average magnitude of the error between observed and predicted values.

To plot and summarize the simulated daily growth rates predicted by the VS model, generalized additive mixed models (GAMMs, Wood, 2017) were fitted on mean Gr to smooth their high intra-annual variability (Valeriano et al., 2021b). The GAMMs were fitted using a restricted maximum likelihood (REML) approach and considering a span of 0.8 using the gam function from the *mgcv* package included in the *ggplot2* R package (Wood, 2011; Wickham, 2016). In the case of daily integral growth rates (GrT, GrW), confidence intervals were also plotted. Finally, we calculated the Hartigan unimodality test or Hartigan's dip statistic (HDS) by the *diptest* R package (Hartigan and Hartigan, 1985; Maechler et al., 2013) and a specific bimodality coefficient (BC, *mousetrap* package; Pfister et al., 2013). The algorithm of HDS evaluates the deviation from unimodality distribution. If the index increases, the distribution deviates from an unimodal distribution indicating significant ($p < 0.05$) bimodality (Maechler et al., 2013). BC takes into the account the sample size and the skewness and kurtosis of the distribution. The values of BC range from 0 to 1, with values closer to 0 indicating strong bimodality (Pfister et al., 2013). For sites with the strongest bimodality according to the HDS and BC, we analysed simulated daily growth rates (Gr) for years with the different spring/autumn precipitation ratios.

3. Results

3.1. Climate patterns

Mean annual temperature of study sites was 13.1 ºC (range 10.1–18.3 ºC) and the average total annual precipitation was 550 mm (range 315–877 mm). The most continental sites were Viloria, Peñaflor, Corbalán, Aliaga and Valonsadero; whereas lower continentality characterized the coastal sites Garraf, Maresme, Prades and Doñana (Table 1, Figs. S1 and S2). Agüero and Napal showed intermediate continentality. The continentality index has increased over time in all study sites, and the steepest trends were found in Corbalán-Aliaga, Peñaflor, Prades and Napal sites (Table 1). In agreement with continentality index, the highest values of the spring/autumn precipitation ratio were found in Valonsadero, Peñaflor, Corbalán, Aliaga, Viloria and Napal, whereas the lowest were found in the easternmost sites Garraf, Maresme, Prades and the Doñana site (Table 1, Fig. 1). In the period 1970–2020, spring/autumn precipitation ratios were unstable: they were low during the 1980 s, 1990 s and mid-2000 s, whereas they were high in the 1970 s and some years in the 2000 s and 2010 s (Fig. 1).

3.2. Growth patterns

Sampled junipers were on average younger (mean age of 67 years) than pines (86 years) (Table 2). All series were well replicated for the common period 1970–2016/2020 according to the EPS. The lowest mean growth rates corresponded to shrubs (*J. phoenicea*), *J. oxycedrus* and *J. communis*, whereas the highest rates corresponded to trees (*P. pinaster* and *P. sylvestris* in Valonsadero; *P. pinaster* in Prades, and *P. halepensis* in Garraf) (Table 2). The highest first-order autocorrelation values were found for *P. pinaster* and *P. sylvestris*. The *P. sylvestris* sites showed the lowest mean sensitivity and the Garraf *P. halepensis* and Maresme *P. pinea* sites showed the highest sensitivity. Lastly, the highest inter-series correlations were found for *P. pinaster* and the lowest for *J. oxycedrus*.

3.3. Relationships between climate and growth

According to climate-growth correlations, wet conditions from winter to summer and cool spring- summer conditions enhanced growth at most sites (Fig. 2). In pines, growth mostly depended on spring precipitation. High winter-spring precipitation improved growth of *J. communis* in Napal and *J. oxycedrus* in Agüero. In *J. thurifera* and *J. phoenicea*, growth was constrained by low summer precipitation. Finally, wet September and October conditions improved growth of *J. thurifera* in Corbalán, *J. phoenicea* in Doñana, *P. pinea* in Maresme and *P. halepensis* in Garraf. Regarding temperature, warm summer conditions limited growth of *P. pinaster*, *J. thurifera* and *J. phoenicea*. Warm September conditions improved growth of *P. halepensis* in Garraf and *J. oxycedrus* in Napal, but limited *P. pinea* growth in Viloria.

3.4. Modelling intra-annual growth

The VS model was able to significantly reproduce chronologies of ring-width indices as a function of climate variability in all study sites and species (Table 3, Fig. S3). According to calibration and verification statistics, the VS model simulations produced a similar year-to-year variability and coherent series of ring-width indices as compared to observed ring-width indices (Table 3).

The highest correlations between observed and simulated series corresponded to *P. pinaster* and *P. sylvestris* in Valonsadero ($r = 0.83$ and $r = 0.85$), whilst the lowest correlations corresponded to *J. thurifera* in Corbalán and *J. oxycedrus* in Napal ($r = 0.51$ and $r = 0.54$; Fig. S3). The highest Glk values were found for *P. sylvestris* in Valonsadero and *J. communis* in Aliaga (90% and 91%), whilst the lowest values were found for *J phoenicea* in Doñana and *J. communis* in Napal (57% and 61%).

3.5. Bimodal growth patterns

Based on the Hartigan unimodality test applied on smoothed daily integral growth rates, the most bimodal species and sites were *P. halepensis* in Garraf, *P. sylvestris* and *P. pinaster* in Prades, *J. phoenicea*

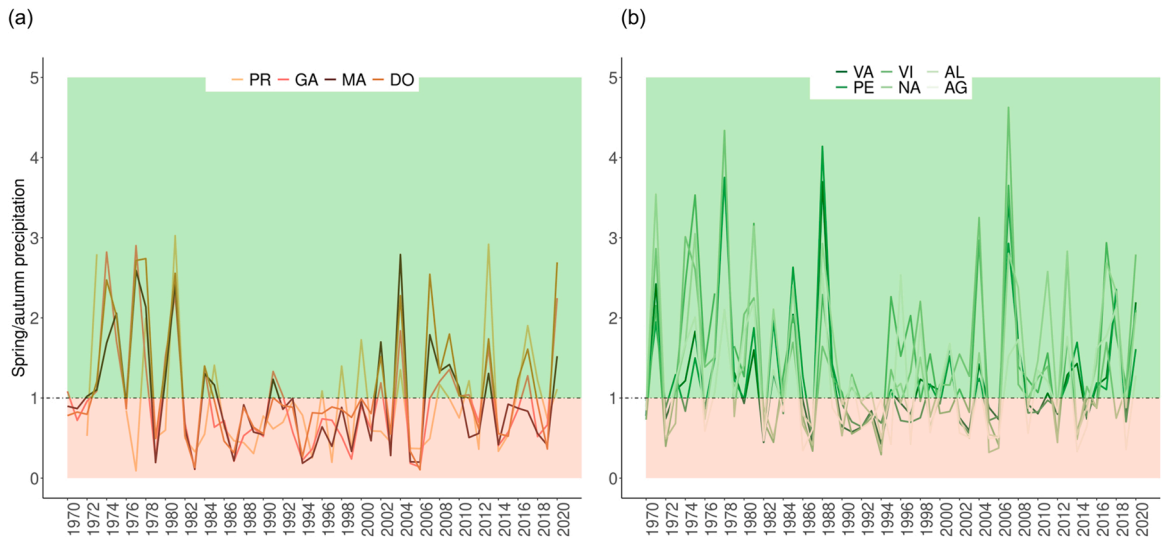

Fig. 1. Ratios between spring and autumn precipitation at sites showing low (a) and high (b) spring/autumn precipitation ratios, respectively (see Table 1). Green and orange areas indicate years with values of the ratio above and below 1, respectively. See sites' codes in Table 1 (AL indicates climate conditions in Aliaga and Corbalán sites).

Table 2
Dendrochronological statistics of eight study species (see sites' codes in Table 1). Variables' abbreviations: EPS, Expressed Population Signal; RW, ring width; SD, standard deviation of ring widths; AR1, first-order autocorrelation; MSx, mean sensitivity; rbar, mean correlation between individuals. Age was estimated at 1.3 m in trees and for basal samples in shrubby junipers (*J. communis*, *J. oxycedrus* and *J. phoenicea*).

Species	Site	No. individuals	No. radii	Age (years)	Period with EPS > 0.85	RW (mm)	SD (mm)	AR1	MSx	rbar
P. sylvestris	PR	42	76	68	1943–2020	1.49	0.84	0.72	0.30	0.64
	VA	15	35	62	1960–2020	3.08	1.67	0.72	0.31	0.68
P. pinaster	PR	23	39	50	1970–2020	2.06	1.72	0.81	0.36	0.78
	VA	20	32	69	1955–2020	3.30	2.42	0.84	0.32	0.74
P. halepensis	GA	24	48	98	1940–2017	1.85	0.92	0.54	0.49	0.72
	PE	38	46	112	1871–2020	0.99	0.66	0.64	0.44	0.75
P. pinea	MA	26	50	104	1946–2020	1.54	1.21	0.52	0.48	0.70
	VI	20	20	124	1914–2016	1.70	1.20	0.56	0.43	0.71
J. communis	NA	14	23	51	1968–2017	0.63	0.32	0.48	0.36	0.46
	AL	15	30	74	1943–2016	1.08	0.47	0.57	0.36	0.47
J. oxycedrus	AG	15	30	70	1947–2020	1.05	0.52	0.58	0.35	0.46
	NA	14	23	76	1943–2017	0.54	0.26	0.50	0.40	0.45
J. thurifera	PE	30	42	61	1970–2020	1.21	0.96	0.62	0.41	0.53
	CO	25	45	82	1944–2020	1.00	0.53	0.63	0.34	0.57
J. phoenicea	PE	16	33	56	1970–2020	0.45	0.23	0.36	0.43	0.48
	DO	42	72	65	1960–2020	0.61	0.31	0.56	0.37	0.52

in Doñana and *P. pinea* in Maresme. Species and sites with less defined bimodality were *J. thurifera* in Peñaflor, *J. communis* in Aliaga and Napal, and *P. pinaster* in Valonsadero (Table 3, Fig. 3). Bimodal sites showed higher growth rates in autumn than their unimodal counterparts and this was very noticeable in *P. halepensis* and *J. phoenicea* (Fig. 3). In these two species the simulated autumn peak reached maximum growth rates about three times higher in the more bimodal sites compared to less bimodal sites. In the other species showing bimodality (*P. sylvestris*, *P. pinaster*, *P. pinea*) the maximum autumn growth rate was twice higher in more bimodal than in less bimodal sites.

In *P. halepensis* and *J. phoenicea* the simulated spring peak reached maximum growth rates about 1.5 times higher in the more bimodal sites as compared with less bimodal sites. The ratio between the spring and autumn maximum growth rates was approximately 2.5 in the most bimodal sites of *P. pinaster*, *P. pinea* and *J. phoenicea*. However, this ratio was slightly lower in *P. sylvestris* (2.0) and *P. halepensis* (1.7), indicating a higher relevance of autumn growth in these two species. In the less bimodal sites, the mean ratio between maximum spring and autumn growth rates was 4.3, but this ratio was higher (5.1) in *P. pinaster* indicating a higher relevance of spring growth in Valonsadero site.

Simulated spring growth peak occurred from early April (*J. phoenicea* in Doñana) to late May (*P. sylvestris* in Valonsadero), whilst the autumn growth peak occurred from early September (*P. sylvestris* in Prades) to late November (*J. phoenicea* in Doñana). Spring and autumn growth peaks occurred (mean ± SD) 9 ± 7 and 24 ± 8 days earlier in more bimodal sites of pine species compared to less bimodal sites. For three of the juniper species, the spring peak occurred for 5 ± 3 earlier in bimodal compared to right-skewed unimodal sites. However, in the case of *J. phoenicea*, the spring peak occurred 19 days earlier, but the autumn peak delayed 28 days in more compared to less bimodal site.

3.6. Climatic drivers of bimodal growth patterns

Radial growth was constrained by low winter temperatures (Fig. 4) and low summer soil moisture in all sites (Fig. 5). Elevated temperatures in summer directly reduced simulated growth for *P. sylvestris* in Prades, *P. pinea* in Maresme, *P. halepensis* at both study sites, *J. communis* in Napal and *J. thurifera* and *J. phoenicea* at both study sites (Fig. 4). The strongest constraining effect of low soil moisture in summer on growth was found for junipers, particularly *J. communis* and *J. thurifera*, but also for *P. pinea* and *P. halepensis* in Peñaflor. At two sites, Agüero and Napal, simulated soil moisture became on average oversaturated for short

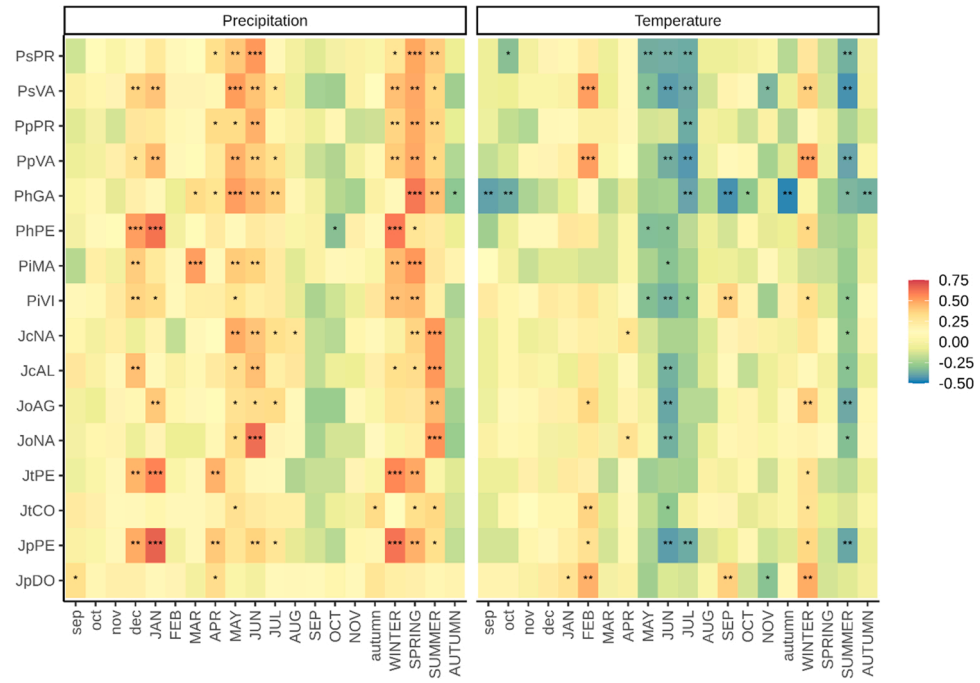

Fig. 2. Climate-growth correlations (color scale) calculated between series of ring-width indices and monthly or seasonal precipitation and temperature data. Months or seasons abbreviated by lowercase or uppercase letters correspond to the prior and current years, respectively. See species' and sites' abbreviations in Table 1 (e.g., PsPR means *P. sylvestris* in Prades site). Significance levels: * $p < 0.05$; * * $p < 0.01$; * ** $p < 0.001$.

Table 3
Process-based growth model statistics of each species and site, the full period correlations are significant for all sites ($p < 0.01$). The synchronicity statistic (Glk) and the root mean square error (RMSE). The last column shows the Hartigan unimodality test index (HDS) with the significance of the test, and bimodality coefficient (BC) of smoothed simulated integral growth rates. Significance levels: * $p < 0.05$, * * $p < 0.01$, N.S. $p > 0.05$.

Species	Site	Period	*r* (Glk, %)	Obs. vs Sim. Chronologies correlation		Glk (%)		RMSE		HDS/BC
				1970–1995	1996–2016/20	1970–1995	1996–2016/2020	1970–1995	1996–2016/2020	
Ps	PR	1970–2020	0.75 (80)	0.75 * *	0.72 * *	76.9	84.0	0.11	0.14	0.04 * */0.62
	VA	1970–2020	0.83 (90)	0.87 * *	0.85 * *	84.6	92.0	0.14	0.14	N.S./0.79
Pp	PR	1970–2020	0.67 (72)	0.66 * *	0.68 * *	76.0	64.0	0.21	0.20	0.03 * */0.68
	VA	1970–2020	0.85 (76)	0.81 * *	0.87 * *	61.5	88.0	0.13	0.13	N.S./0.84
Ph	GA	1970–2016	0.72 (85)	0.65 * *	0.83 * *	76.9	90.9	0.19	0.11	0.04 * */0.59
	PE	1970–2020	0.66 (74)	0.72 * *	0.68 * *	73.1	72.0	0.23	0.26	N.S./0.83
Pi	MA	1970–2020	0.79 (86)	0.73 * *	0.88 * *	84.6	84.0	0.31	0.26	0.01 * /0.70
	VI	1970–2016	0.57 (81)	0.64 * *	0.39 *	76.9	80.9	0.35	0.42	N.S./0.82
Jc	NA	1985–2016	0.59 (61)	0.80 * *	0.50 * *	68.7	47.1	0.22	0.23	N.S./0.81
	AL	1985–2016	0.82 (91)	0.85 * *	0.81 * *	87.5	87.5	0.30	0.15	N.S./0.84
Jo	AG	1985–2016	0.62 (78)	0.67 * *	0.65 * *	75.0	65.0	0.15	0.19	N.S./0.78
	NA	1985–2016	0.54 (70)	0.66 * *	0.67 * *	76.5	52.9	0.20	0.24	N.S./0.72
Jt	PE	1970–2020	0.64 (71)	0.61 * *	0.69 * *	69.2	68.0	0.20	0.19	N.S./0.83
	CO	1970–2020	0.51 (72)	0.42 *	0.77 * *	57.7	87.5	0.34	0.20	N.S./0.85
Jp	PE	1970–2020	0.76 (76)	0.74 * *	0.78 * *	53.9	80.0	0.27	0.23	N.S./0.82
	DO	1970–2020	0.63 (57)	0.53 * *	0.71 * *	46.1	60.0	0.19	0.14	0.02 * */0.65

periods during spring; this effect could be due to elevated precipitation in winter season and high soil water holding capacity (Fig. 5). In the case of *P. sylvestris*, stronger growth limitations due to low summer soil moisture were found in Valonsadero as compared with Prades, where autumn precipitation alleviated summer stress due to drought and high temperatures (Table 1, Fig. S2).

The bimodal pattern strengthened in years with higher autumn than spring precipitation in: *P. sylvestris* and *P. pinaster* in Prades, *P. halepensis* in Garraf, *P. pinea* in Maresme and *J. phoenicea* in Doñana (Fig. 6, Fig. S4). The autumn peak in these species and sites was produced, according to VS model simulations, by alleviation of late summer drought stress due to increased soil moisture levels from late September until late November (Fig. S4).

4. Discussion

For each tree species, bimodal growth patterns were more evident in coastal sites with mild climate (e.g., *P. halepensis* in Garraf, *P. sylvestris* and *P. pinaster* in Prades, *P. pinea* in Maresme and *J. phoenicea* in Doñana). Thus, facultative bimodal growth patterns of gymnosperm trees and shrubs can occur if autumn precipitation is sufficient to reactivate cambial activity after summer quiescence. As continentality increases and autumn precipitation decreases, bimodality diminishes (Pasho et al., 2012; Vieira et al., 2014).

Our simulations based on the VS model agree with previous growth phenology analyses based on dendrometer and xylogenesis data (Camarero et al., 2010; Campelo et al., 2021b, 2018; Gutiérrez et al., 2011; Pacheco et al., 2018; Vieira et al., 2015). In coastal sites with mild climate conditions (low continentality degree) and sufficient autumn

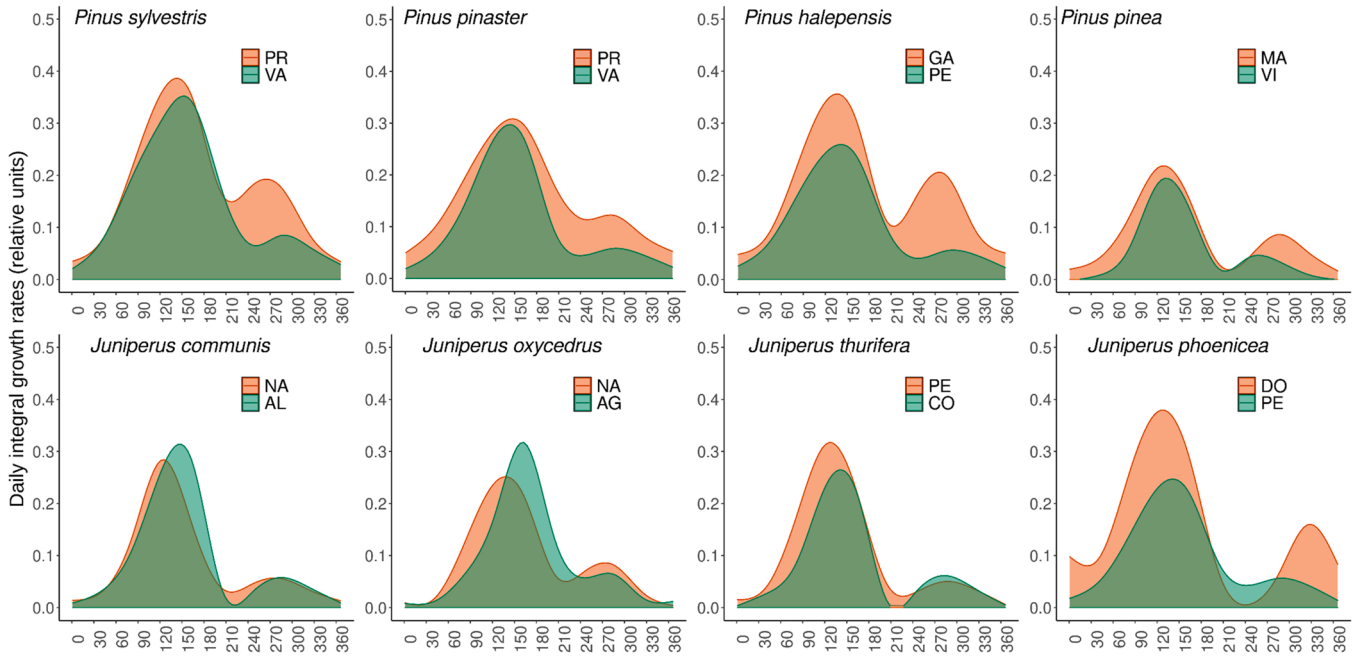

Fig. 3. Daily integral growth rates obtained by fitting the VS model for the period 1970/85–2016/2020 (for specific chronologies spans, see Table 3) and smoothed using GAMMs for eight study species. Orange and green areas correspond to more and less bimodal sites for each species.

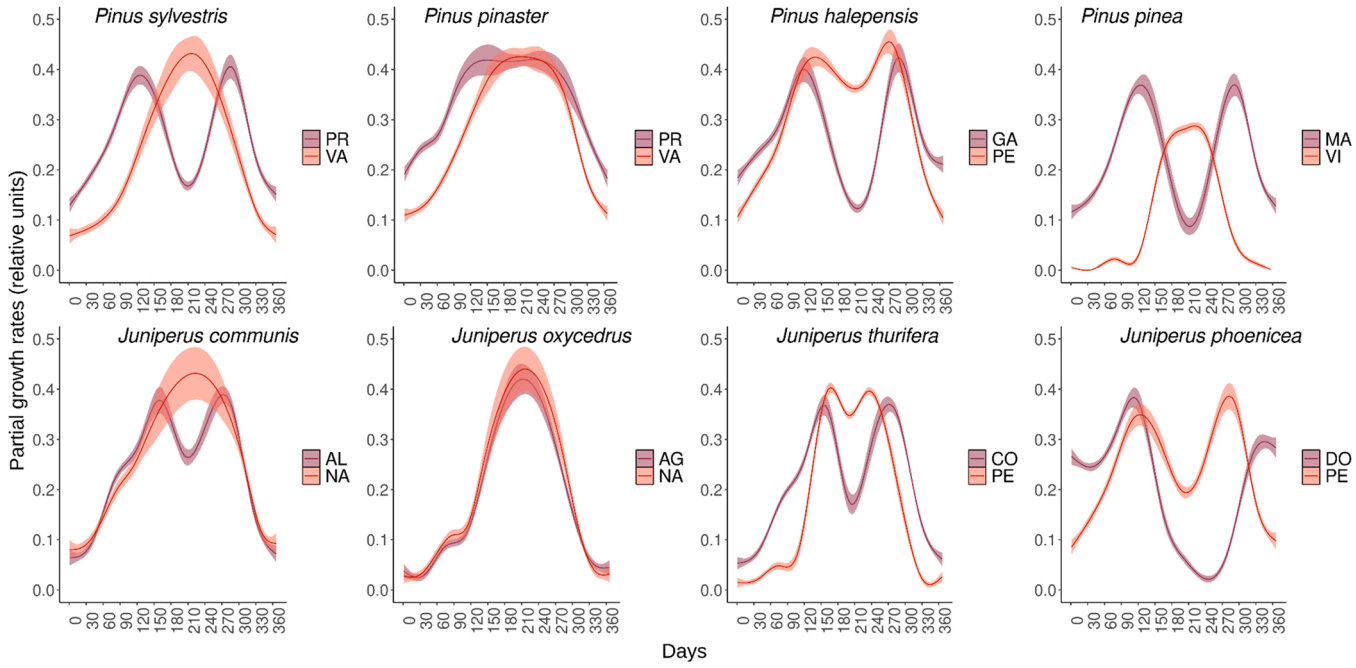

Fig. 4. Mean growth dependence on temperature (GrT) during the year for individual sites. Note that lower values in the y axes (partial growth rates dependence on temperature) indicate stronger limitation of growth by low (winter) or high temperature (summer). See sites' codes in Table 1.

precipitation, trees can restart growth after the summer quiescence period and produce a second growth peak. Trees in coastal sites have been shown to resume cambial activity in autumn after periods of minimum growth during the dry summer as observed in *P. halepensis* (Pacheco et al., 2018), *P. pinaster* (Carvalho et al., 2015; Vieira et al., 2020) or in *Pinus nigra* Arn. (Szymczak et al., 2020). However, this response depends on site climate conditions since elevated temperatures and low soil moisture constrain cambial activity by reducing turgor and cambial division and could lead to unimodal growth patterns (Häusser et al., 2021). Finally, shifts in the spring/autumn precipitation ratio affected bimodality strength, for instance, in the case of *J. phoenicea* in Doñana, which may be due to the shallow depth of its roots and the type of sandy soil in the dunes (Fig. 1). However, changes in the level of bimodality between years were minor in the case of *P. halepensis* in Garraf where the autumn precipitation peak occurs most years (Table 3). Thus, year-to-year seasonal precipitation variability should be also accounted for when studying growth bimodality.

In this regard, juniper species seem to display a more bimodal pattern when coexisting with pine species in semi-arid locations as observed in *J. thurifera* and *P. halepensis* (Camarero et al., 2010; Tumajer

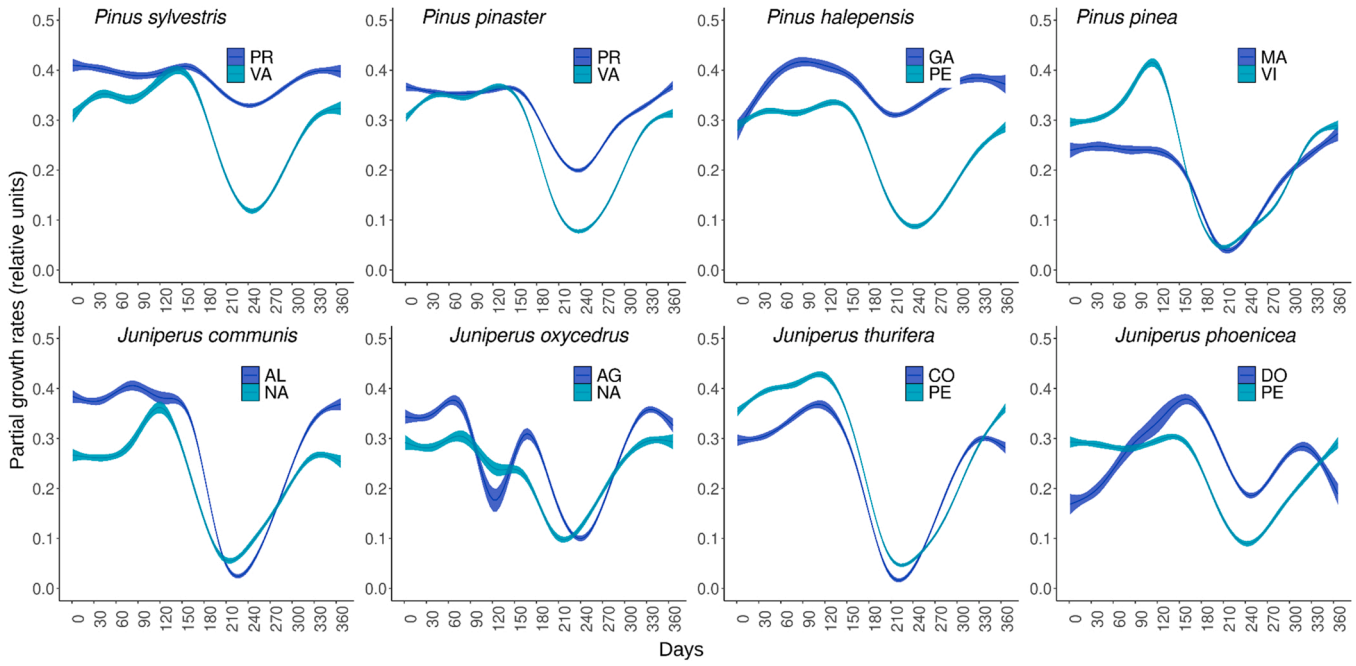

Fig. 5. Mean growth dependence on soil moisture (GrW) during the year for individual sites. Note that lower values in the y axes (partial growth rates dependence on soil moisture) indicate stronger limitation of growth by soil moisture availability. See sites' codes in Table 1.

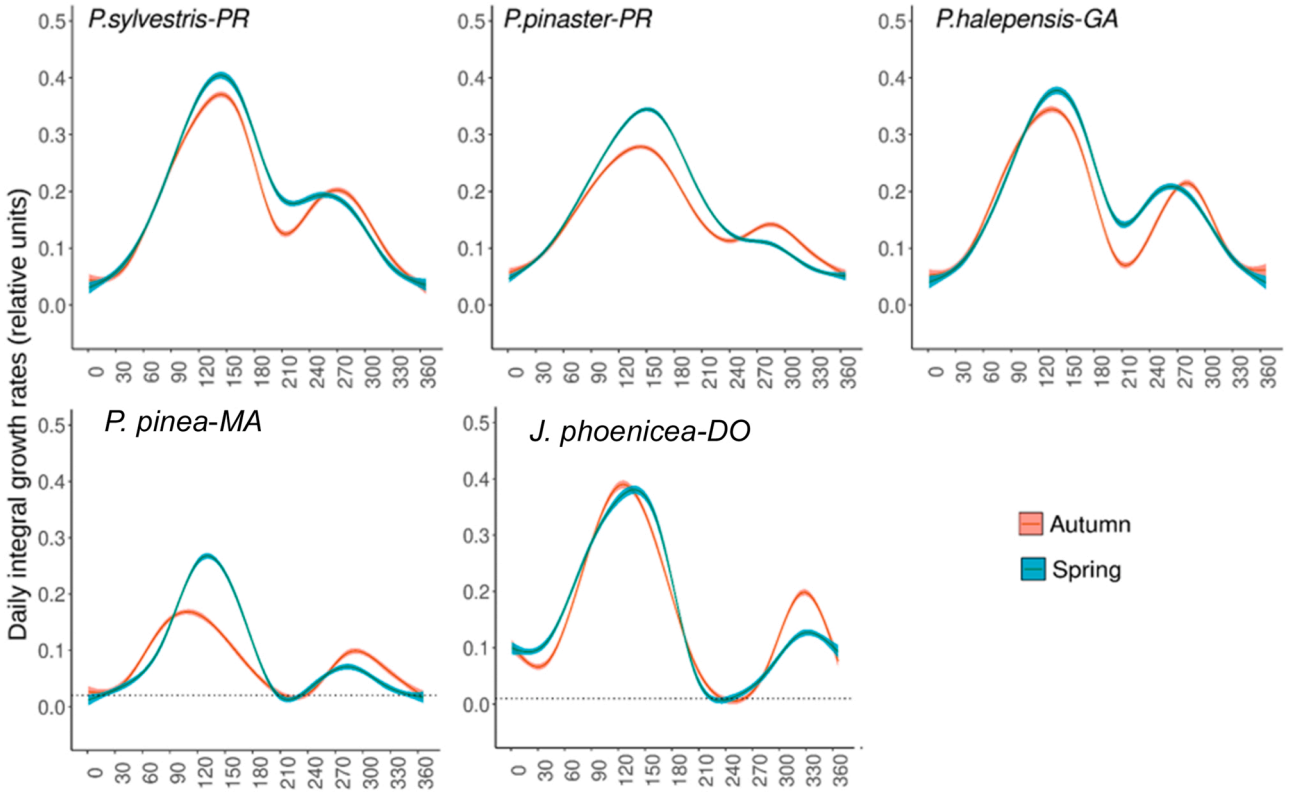

Fig. 6. Simulated growth rates for the species with the most marked bimodality showing differences in growth patterns between sites. Values of simulated integral growth rates were smoothed using GAMM. Intra-annual patterns of growth rates are shown for years with autumn precipitation higher than spring precipitation (autumn, orange lines) and vice versa (spring, blue lines).

et al., 2021b). In that case the pine was able to keep some minimum growth levels in summer, perhaps due to higher hydraulic conductivity and gas exchange rate (Borghetti et al., 1998), whereas the autumn regrowth peak was stronger in the juniper (Camarero et al., 2021a). Therefore, studies considering several coexisting tree and shrub species could also address how they adjust bimodality to tolerate summer drought.

The climate-growth correlations did not highlight a prominent role

of autumn conditions on annual radial growth (Fig. 2). This may be explained because most of the annual ring is formed in spring and the influence of autumn conditions on xylogenesis may be episodic and depend on site and climate conditions (Camarero et al., 2010). At most sites, growth positively correlated with wet winter-spring conditions and cool spring-summer conditions which improve earlywood production and radial growth in Mediterranean woody plants (Pasho et al., 2011). We could only detect positive correlations between September and October precipitation and growth in the bimodal *P. pinea* (Maresme) and *J. phoenicea* (Doñana) sites, locations with shallow soil depth and sandy soils. Indeed, these relationships could be due to carry-over effects between winter-to-spring precipitation and developing wood anatomy (early and latewood). Latewood development dependence on autumn climate has been observed in *P. halepensis* (Pacheco et al., 2018) and *P. pinea* (Castagneri et al., 2018). Overall, simulated spring growth peaks were always more important in absolute terms, reaching higher growth rates, than autumn growth peaks (Fig. 6).

We argue that further species and regions should be screened for bimodal growth patterns. To enlarge available datasets, such screening could involve simulations produced by established or new process-based models. Our study supports the use of the VS model under Mediterranean conditions, because it produced simulated chronologies with highly significant correlations with observed chronologies at all study sites (Table 3). However, model outputs should be backed up and verified by ground observations of seasonal growth based either on xylogenesis or dendrometer data (e.g., Camarero et al., 2010; Pacheco et al., 2018; Tumajer et al., 2021b). In other words, intra-annual simulations of growth should be calibrated by long-term xylogenesis or dendrometer data which would improve parameter tuning (cf. Tumajer et al., 2021a). For instance, such tuning should verify simulated intra-annual growth kinetics and dates of cambium activity onset and cessation which in Mediterranean conditions depend on surpassing a minimum temperature or a soil moisture threshold (e.g., Ren et al., 2018).

Regarding future investigations on radial growth bimodality it is essential: (i) to disentangle if autumn radial increment is actual radial growth or stem swelling due to rehydration of stem tissues after summer drought (Mäkinen et al., 2008; Zweifel et al., 2016), and (ii) to discern to what extent bimodal growth is triggered by climatic drivers, as dendrochronological studies assume (Camarero et al., 2010; Campelo et al., 2021; Pacheco et al., 2016, 2018; Tumajer et al., 2021b) and dendrometer data show (Vieira et al., 2013), and to what extent it depends on internal processes (De Micco et al., 2016). Although climate-driven process-based models can deepen our understanding of spatial and between-species variability in simulated bimodality (Touchan et al., 2012), due to their assumptions they cannot provide answers to those essential questions, that need to be addressed by empirical or experimental studies. For example, in a recent experiment with *P. sylvestris*, the autumn growth peak was induced by girdling, blocking phloem fluxes and shifting carbon allocation (Oberhuber et al., 2021). It could be further investigated how changes in carbon allocation and plant hydraulic functioning depend on changes in soil water availability, xylogenesis and bimodal growth (Garcia-Forner et al., 2019). The use of process-based models to forecast tree growth and vigor (e.g., Sánchez-Salguero et al., 2017a; 2017b) should consider bimodal patterns and predict growth seasonality as a function of climate scenarios. For instance, our approach could be used to better understand if warmer and more continental conditions observed across central Spain since the 1980s lead to growth decline and increased vulnerability to drought-induced dieback in some tree and shrub species (Sánchez-Salguero and Camarero, 2020; Valeriano et al., 2021b). Further studies could focus on searching for bimodal growth patterns in other tree and shrub populations subjected to diverse climate constraints. Last but not least, bimodality should be integrated into forecasts to assess if shifting bimodality will improve post-drought recovery in response to wet autumn conditions.

5. Conclusions

We found stronger bimodal growth patterns in coastal, less continental sites with abundant autumn precipitation of several tree (*P. halepensis*, *P. sylvestris*, *P. pinaster*, *P. pinea*) and shrub (*J. phoenicea*) species. Bimodal patterns varied between sites, species and over time and reflected spring/autumn precipitation ratios. Since spring growth rates were always higher than autumn rates, bimodality could play a secondary role for improving growth resilience after summer drought. This could favour latewood formation and carbon fixation in tracheid cell walls through higher autumn growth rates and longer growing season, representing a crucial adaptation of woody plants for withstanding seasonally dry climates.

Funding

This work was supported by project RTI2018–096884-B-C31 and by FPI grant (ref. PRE2019–089800) to CV from the Spanish Ministry of Science. RSS was supported by DendrOlavide I (EQC2018–005303-P), Ministry of Science, Innovation and Universities, Spain; DendrOlavide II (IE19_074 UPO), VURECLIM (P20_00813) and VULBOS (UPO-1263216) Junta de Andalucía, Fondos Europeos de Desarrollo Regional. JT received the support from Charles University (UNCE/HUM 018). VS was grateful for the support of RSF project (# 22–14–00048).

Declaration of Competing Interest

The authors declare that they have no known competing financial interests or personal relationships that could have appeared to influence the work reported in this paper.

Data Availability

The data that support the findings of this study are available on request from the corresponding author.

Acknowledgements

We acknowledge the E OBS dataset from the EU-FP6 project UERRA (http://www.uerra.eu) and the data providers in the ECA&D project (https://www.ecad.eu). We thank J. Oliva for providing Maresme samples.

Appendix A. Supporting information

Supplementary data associated with this article can be found in the online version at doi:10.1016/j.dendro.2023.126057.

References

Andrade, C., Corte-Real, J.A., 2015. Preliminary assessment of aridity conditions in the Iberian Peninsula. AIP Conf. Proc. 1738, 060003 https://doi.org/10.1063/1.4912413.

Battipaglia, G., de Micco, V., Brand, W.A., Linke, P., Aronne, G., Saurer, M., Cherubini, P., 2010. Variations of vessel diameter and δ13C in false rings of *Arbutus unedo* L. reflect different environmental conditions. N. Phytol. 188, 1099–1112. https://doi.org/10.1111/J.1469-8137.2010.03443.X.

Battipaglia, G., Campelo, F., Vieira, J., Grabner, M., De Micco, V., Nabais, C., Cherubini, P., Carrer, M., Bräuning, A., Čufar, K., Di Filippo, A., García-González, I., Koprowski, M., Klisz, M., Kirdyanov, A.V., Zafirov, N., de Luis, M.M., 2016. Structure and function of intra-annual density fluctuations: mind the gaps. Front. Plant Sci. 7, 595. https://doi.org/10.3389/fpls.2016.00595.

Borghetti, M., Cinnirella, S., Magnani, F., Saracino, A., 1998. Impact of long-term drought on xylem embolism and growth in *Pinus halepensis* Mill. Trees Struct. Funct. 12, 187–195. https://doi.org/10.1007/PL00009709.

Bunn, A.G., 2010. Statistical and visual crossdating in R using the dplR library. Dendrochronologia 28, 251–258. https://doi.org/10.1016/J.DENDRO.2009.12.001.

Bunn, A.G., 2021. dplR: Dendrochronology Program Library in R. R package version 1.7.2. ⟨https://CRAN.R-project.org/package=dplR⟩.

Buras, A., Wilmking, M., 2015. Correcting the calculation of Gleichläufigkeit. Dendrochronologia 34, 29–30. https://doi.org/10.1016/J.DENDRO.2015.03.003.

Camarero, J.J., Olano, J.M., Parras, A., 2010. Plastic bimodal xylogenesis in conifers from continental Mediterranean climates. N. Phytol. 185, 471–480. https://doi.org/10.1111/J.1469-8137.2009.03073.X.

Camarero, J.J., Gazol, A., Sangüesa-Barreda, G., Oliva, J., Vicente-Serrano, S.M., 2015. To die or not to die: early warnings of tree dieback in response to a severe drought. J. Ecol. 103, 44–57. https://doi.org/10.1111/1365-2745.12295.

Camarero, J.J., Gazol, A., Sánchez-Salguero, R., Sangüesa-Barreda, G., Díaz-Delgado, R., Casals, P., 2020. Dieback and mortality of junipers caused by drought: dissimilar growth and wood isotope patterns preceding shrub death. Agric. For. Meteorol. 291, 108798 https://doi.org/10.1016/j.agrformet.2020.108078.

Camarero, J.J., Rubio-Cuadrado, A., Gazol, A., 2021a. Climate windows of intra-annual growth and post-drought recovery in Mediterranean trees. Agric. For. Meteorol. 308, 108606 https://doi.org/10.1016/j.agrformet.2021.108606.

Camarero, J.J., Valeriano, C., Gazol, A., Colangelo, M., Sánchez-Salguero, R., 2021b. Climate differently impacts the growth of coexisting trees and shrubs under semi-arid Mediterranean conditions. Forests 12, 381. https://doi.org/10.3390/f12030381.

Campelo, F., Gutiérrez, E., Ribas, M., Sánchez-Salguero, R., Nabais, C., Camarero, J.J., 2018. The facultative bimodal growth pattern in *Quercus ilex* – a simple model to predict sub-seasonal and inter-annual growth. Dendrochronologia 49, 77–88. https://doi.org/10.1016/j.dendro.2018.03.001.

Campelo, F., Ribas, M., Gutiérrez, E., 2021. Plastic bimodal growth in a Mediterranean mixed-forest of *Quercus ilex* and *Pinus halepensis*. Dendrochronologia 67, 125836. https://doi.org/10.1016/j.dendro.2021.125836.

Carvalho, A., Nabais, C., Vieira, J., Rossi, S., Campelo, F., 2015. Plastic response of tracheids in *Pinus pinaster* in a water-limited environment: adjusting lumen size instead of wall thickness. PLoS One 10, 1–14. https://doi.org/10.1371/journal.Pone.0136305.

Castagneri, D., Battipaglia, G., von Arx, G., Pacheco, A., Carrer, M., 2018. Tree-ring anatomy and carbon isotope ratio show both direct and legacy effects of climate on bimodal xylem formation in *Pinus pinea*. Tree Physiol. 38, 1098–1109. https://doi.org/10.1093/treephys/tpy036.

Cherubini, P., Gartner, B.L., Tognetti, R., Bräker, O.U., Schoch, W., Innes, J.L., 2003. Identification, measurement and interpretation of tree rings in woody species from mediterranean climates. Biol. Rev. 78, 119–148. https://doi.org/10.1017/S1464793102006000.

Collado, E., Bonet, J.A., Camarero, J.J., Egli, S., Peter, M., Salo, K., Martínez-Peña, F., Ohenoja, E., Martín-Pinto, P., Primicia, I., Büntgen, U., Kurttila, M., Oria-de-Rueda, J.A., Martínez-de-Aragón, J., Miina, J., de-Miguel, S., 2019. Mushroom productivity trends in relation to tree growth and climate across different European forest biomes. Sci. Total Environ. 689, 602–615. https://doi.org/10.1016/J.SCITOTENV.2019.06.471.

Cook, E.R., Kairiukstis, L.A., 1990. Methods of Dendrochronology: Application in the Environmental Science. Kluwer, Dordrecht.

Cornes, R.C., van der Schrier, G., van den Besselaar, E.J.M., Jones, P.D., 2018. An ensemble version of the E-OBS temperature and precipitation data sets. J. Geophys. Res.: Atmos. 123, 9391–9409. https://doi.org/10.1029/2017JD028200.

Cuny, H.E., Rathgeber, C.K., Frank, D., Fonti, P., Mäkinen, H., et al., 2015. Woody biomass production lags stem-girth increase by over one month in coniferous forests. Nat. Plants 1, 15160. https://doi.org/10.1038/NPLANTS.2015.160.

De Luis, M., Gričar, J., Čufar, K., Raventós, J., 2007. Seasonal dynamics of wood formation in *Pinus halepensis* from dry and semi-arid ecosystems in Spain. IAWA J. 28, 389–404. https://doi.org/10.1163/22941932-90001651.

De Luis, M., Novak, K., Raventós, J., Gričar, J., Prislan, P., Čufar, K., 2011. Cambial activity, wood formation and sapling survival of *Pinus halepensis* exposed to different irrigation regimes. For. Ecol. Manag. 262, 1630–1638. https://doi.org/10.1016/j.foreco.2011.07.013.

De Micco, V., Balzano, A., Čufar, K., Aronne, G., Gričar, J., Merela, M., Battipaglia, G., 2016. Timing of false ring formation in *Pinus halepensis* and *Arbutus unedo* in southern Italy: Outlook from an analysis of xylogenesis and tree-ring chronologies. Front. Plant Sci. 7, 1–14. https://doi.org/10.3389/fpls.2016.00705.

Del Río, M., Rodríguez-Alonso, J., Bravo-Oviedo, A., Ruíz-Peinado, R., Cañellas, I., Gutiérrez, E., 2014. Aleppo pine vulnerability to climate stress is independent of site productivity of forest stands in southeastern Spain. Trees Struct. Funct. 28, 1209–1224. https://doi.org/10.1007/s00468-014-1031-0.

Delpierre, N., Lireux, S., Hartig, F., Camarero, J.J., Cheaib, A., et al., 2019. Chilling and forcing temperatures interact to predict the onset of wood formation in Northern Hemisphere conifers. Glob. Change Biol. 25, 1089–1105. https://doi.org/10.1111/GCB.14539.

Fritts, H.C., 1976. Tree Rings and Climate. Academic Press, London, UK.

Garcia-Forner, N., Vieira, J., Nabais, C., Carvalho, A., Martínez-Vilalta, J., Campelo, F., 2019. Climatic and physiological regulation of the bimodal xylem formation pattern in *Pinus pinaster* saplings. Tree Physiol. 39, 2008–2018. https://doi.org/10.1093/treephys/tpz099.

Gazol, A., Camarero, J.J., 2012. Mediterranean dwarf shrubs and coexisting trees present different radial-growth synchronies and responses to climate. Plant Ecol. 213, 1687–1698. https://doi.org/10.1007/s11258-012-0124-3.

Gazol, A., Ribas, M., Gutiérrez, E., Camarero, J.J., 2017. Aleppo pine forests from across Spain show drought-induced growth decline and partial recovery. Agric. For. Meteorol. 232, 186–194. https://doi.org/10.1016/J.AGRFORMET.2016.08.014.

Génova, M., Sánchez-Espejo, J., Domínguez-Lozano, F., Moreno-Saiz, J.C., 2013. Dendrochronological study of the endangered shrub *Vella pseudocytisus* subsp. paui (Brassicaceae): implications for its recovery and conservation. An. Del. Jardín Botánico De. Madr. 70, 178–186.

Gordo, O., Sanz, J.J., 2005. Phenology and climate change: a long-term study in a Mediterranean locality. Oecologia 146, 484–495. https://doi.org/10.1007/S00442-005-0240-Z/FIGURES/6.

Gordo, O., Sanz, J.J., 2009. Long-term temporal changes of plant phenology in the Western Mediterranean. Glob. Change Biol. 15, 1930–1948. https://doi.org/10.1111/J.1365-2486.2009.01851.X.

Gutiérrez, E., Campelo, F., Camarero, J.J., Ribas, M., Muntán, E., Nabais, C., Freitas, H., 2011. Climate controls act at different scales on the seasonal pattern of *Quercus ilex* L. stem radial increments in NE Spain. Trees Struct. Funct. 25, 637–646. https://doi.org/10.1007/S00468-011-0540-3/FIGURES/6.

Hartigan, J.A., Hartigan, P.M., 1985. The dip test of unimodality. Ann. Stat. 13, 70–84.

Häusser, M., Szymczak, S., Knerr, I., Bendix, J., Garel, E., Huneau, F., Trachte, K., Santoni, S., Bräuning, A., 2021. The dry and the wet case: tree growth response in climatologically contrasting years on the island of Corsica. Forests 2021 Vol. 12, 1175. https://doi.org/10.3390/F12091175.

He, Z., Du, J., Chen, L., Zhu, X., Lin, P., Zhao, M., Fang, S., 2018. Impacts of recent climate extremes on spring phenology in arid-mountain ecosystems in China. Agric. For. Meteorol. 260, 31–40. https://doi.org/10.1016/j.agrformet.2018.05.022.

Holmes, R., 1983. Computer-assisted quality control in tree-ring dating and measurement. Tree Ring Bull. 43, 69–78.

Larsson L., Larsson P., 2018 CooRecorder/CDendro package version 9.3.1. Cybis, Saltsjöbaden, Sweden.

Lempereur, M., Martin-Stpaul, N.K., Damesin, C., Joffre, R., Ourcival, J.-M., Rocheteau, A., Rambal, S., 2015. Growth duration is a better predictor of stem increment than carbon supply in a Mediterranean oak forest: implications for assessing forest productivity under climate change. N. Phytol. 207, 579–590. https://doi.org/10.1111/nph.13400.

Liphschitz, N., Lev-Yadun, S., Rosen, E., Waisel, Y., 1984. The annual rhythm of activity of the lateral meristems (cambium and phellogen) in *Pinus halepensis* Mill. and *Pinus pinea* L. IAWA J. 5 (4), 263–274. https://doi.org/10.1163/22941932-90000413.

Liu, X., Nie, Y., Wen, F., 2018. Seasonal dynamics of stem radial increment of *Pinus taiwanensis* Hayata and its response to environmental factors in the Lushan Mountains, Southeastern China. Forests 2018 9, 387. https://doi.org/10.3390/F9070387.

Maechler, M., 2013. Package 'diptest'. R Package Version 0–0.76. R: a language and environment for statistical computing. Vienna, Austria: R Foundation for Statistical Computing.

Mäkinen, H., Seo, J.W., Nöjd, P., Schmitt, U., Jalkanen, R., 2008. Seasonal dynamics of wood formation: a comparison between pinning, microcoring and dendrometer measurements. Eur. J. For. Res. 127 (3), 235–245. https://doi.org/10.1007/s10342-007-0199-x.

Martín-Vide. J., Olcina, J. 2001. Climas y tiempos de España. Alianza Ed., Barcelona, Spain.

Menzel, A., Sparks, T.H., Estrella, N., Koch, E., Aaasa, A., Ahas, R., et al., 2006. European phenological response to climate change matches the warming pattern. Glob. Change Biol. 12, 1969–1976. https://doi.org/10.1111/J.1365-2486.2006.01193.X.

Mitrakos, K., 1980. A theory for mediterranean plant life. Acta Oecol./ Oecol. Plant. 1, 245–252.

Morino, K., Minor, R.L., Barron-Gafford, G.A., Brown, P.M., Hughes, M.K., 2021. Bimodal cambial activity and false-ring formation in conifers under a monsoon climate. Tree Physiol. 41, 1893–1905. https://doi.org/10.1093/treephys/tpab045.

Oberhuber, W., Landlinger-Weilbold, A., Schröter, D.M., 2021. Triggering bimodal radial stem growth in pinus sylvestris at a drought-prone site by manipulating stem carbon availability. Front. Plant Sci. 12, 799. https://doi.org/10.3389/FPLS.2021.674438/BIBTEX.

Pacheco, A., Camarero, J.J., Carrer, M., 2016. Linking wood anatomy and xylogenesis allows pinpointing of climate and drought influences on growth of coexisting conifers in continental Mediterranean climate. Tree Physiol. 36, 502–512. https://doi.org/10.1093/TREEPHYS/TPV125.

Pacheco, A., Camarero, J.J., Ribas, M., Gazol, A., Gutierrez, E., Carrer, M., 2018. Disentangling the climate-driven bimodal growth pattern in coastal and continental Mediterranean pine stands. Sci. Total Environ. 615, 1518–1526. https://doi.org/10.1016/J.SCITOTENV.2017.09.133.

Pasho, E., Camarero, J.J., de Luis, M., Vicente-Serrano, S.M., 2011. Impacts of drought at different time scales on forest growth across a wide climatic gradient in north-eastern Spain. Agric. For. Meteorol. 151, 1800–1811. https://doi.org/10.1016/J.AGRFORMET.2011.07.018.

Pasho, E., Camarero, J.J., Vicente-Serrano, S.M., 2012. Climatic impacts and drought control of radial growth and seasonal wood formation in *Pinus halepensis*. Trees 26 (6), 1875–1886. https://doi.org/10.1007/s00468-012-0756-x.

Pellizzari, E., Camarero, J.J., Gazol, A., Granda, E., Shetti, R., Wilmking, M., Moiseev, P., Pividori, M., Carrer, M., 2017. Diverging shrub and tree growth from the Polar to the Mediterranean biomes across the European continent. Glob. Change Biol. 23, 3169–3180. https://doi.org/10.1111/GCB.13577.

Pendergrass, A.G., Knutti, R., Lehner, F., Deser, C., Sanderson, B.M., 2017. Precipitation variability increases in a warmer climate. Sci. Rep. 7, 1–9. https://doi.org/10.1038/s41598-017-17966-y.

Peñuelas, J., Filella, I., Comas, P., 2002. Changed plant and animal life cycles from 1952 to 2000 in the Mediterranean region. Glob. Change Biol. 8, 531–544. https://doi.org/10.1046/J.1365-2486.2002.00489.X.

Peñuelas, J., Filella, I., Zhang, X., Llorens, L., Ogaya, R., Lloret, F., Comas, P., Estiarte, M., Terradas, J., 2004. Complex spatiotemporal phenological shifts as a response to rainfall changes. N. Phytol. 161, 837–846. https://doi.org/10.1111/j.1469-8137.2003.01003.x.

Pfister, R., Schwarz, K.A., Janczyk, M., Dale, R., Freeman, J.B., 2013. Good things peak in pairs: a note on the bimodality coefficient. Front. Psychol. 4, 700. https://doi.org/10.3389/FPSYG.2013.00700/BIBTEX.

Pompa-García, M., Camarero, J.J., Colangelo, M., Gallardo-Salazar, J.L., 2021. Xylogenesis is uncoupled from forest productivity. Trees Struct. Funct. 35, 1123–1134. https://doi.org/10.1007/S00468-021-02102-1/TABLES/1.

Quero, J.L., Sterck, F.J., Martínez-Vilalta, J., Villar, R., 2011. Water-use strategies of six co-existing Mediterranean woody species during a summer drought. Oecologia 166, 45–57. https://doi.org/10.1007/s00442-011-1922-3.

R Development Core Team. 2022. R: A Language and Environment for Statistical Computing.

Ren, P., Rossi, S., Camarero, J.J., Ellison, A.M., Liang, E., Peñuelas, J., 2018. Critical temperature and precipitation thresholds for the onset of xylogenesis of Juniperus przewalskii in a semi-arid area of the north-eastern Tibetan Plateau. Ann. Bot. 121, 617–624. https://doi.org/10.1093/AOB/MCX188.

Sánchez-Salguero, R., Camarero, J.J., 2020. Greater sensitivity to hotter droughts underlies juniper dieback and mortality in Mediterranean shrublands. Sci. Total Environ. 721, 137599 https://doi.org/10.1016/j.scitotenv.2020.137599.

Sánchez-Salguero, R., Camarero, J.J., Carrer, M., Gutiérrez, E., Alla, A.Q., Andreu-Hayles, L., Hevia, A., Koutavas, A., Martínez-Sancho, E., Nola, P., Papadopoulos, A., Pasho, E., Toromani, E., Carreira, J.A., Linares, J.C., 2017a. Climate extremes and predicted warming threaten Mediterranean Holocene firs forests refugia. PNAS 114, E10142–E10150. https://doi.org/10.1594/PANGAEA.882101.

Sánchez-Salguero, R., Camarero, J.J., Gutiérrez, E., González Rouco, F., Gazol, A., Sangüesa-Barreda, G., Andreu-Hayles, L., Linares, J.C., Seftigen, K., 2017b. Assessing forest vulnerability to climate warming using a process-based model of tree growth: bad prospects for rear-edges. Glob. Change Biol. 23, 2705–2719. https://doi.org/10.1111/GCB.13541.

Shishov, V.V., Tychkov, I.I., Popkova, M.I., Ilyin, V.A., Bryukhanova, M.V., Kirdyanov, A.V., 2016. VS-oscilloscope: a new tool to parameterize tree radial growth based on climate conditions. Dendrochronologia 39, 42–50.

Shishov, V.V., Tychkov, I.I., Anchukaitis, K.J., Zelenov, G.K., Vaganov, E.A., 2021. Band model of cambium development: opportunities and prospects. Forests 12, 1361. https://doi.org/10.3390/f12101361.

Szymczak, S., Häusser, M., Garel, E., Santoni, S., Huneau, F., Knerr, I., Trachte, K., Bendix, J., Bräuning, A., 2020. How do Mediterranean pine trees respond to drought and precipitation events along an elevation gradient. Forests 11, 758. https://doi.org/10.3390/F11070758.

Thornthwaite, C.W., Mather, J.R., 1955. The water balance, publication in climatology. Climatology 8, 104. Centeron NJ: Drexel Institute of Technology.

Touchan, R., Shishov, V. v, Meko, D.M., Nouiri, I., Grachev, A., 2012. Process based model sheds light on climate sensitivity of Mediterranean tree-ring width. Biogeosciences 9, 965–972. https://doi.org/10.5194/BG-9-965-2012.

Tumajer, J., Kašpar, J., Kuželová, H., Shishov, V. v, Tychkov, I.I., Popkova, M.I., Vaganov, E.A., Treml, V., 2021a. Forward modeling reveals multidecadal trends in cambial kinetics and phenology at treeline. Front. Plant Sci. 12, 32. https://doi.org/10.3389/fpls.2021.613643.

Tumajer, J., Shishov, V. v, Ilyin, V.A., Camarero, J.J., 2021b. Intra-annual growth dynamics of Mediterranean pines and junipers determines their climatic adaptability. Agric. For. Meteorol. 311, 108685 https://doi.org/10.1016/J.AGRFORMET.2021.108685.

Tumajer, J., Buras, A., Camarero, J.J., Carrer, M., Shetti, R., Wilmking, M., Altman, J., Sangüesa-Barreda, G., Lehejček, J., 2021c. Growing faster, longer or both? Modelling plastic response of *Juniperus communis* growth phenology to climate change. Glob. Ecol. Biogeogr. 30, 2229–2244. https://doi.org/10.1111/geb.13377.

Tychkov, I.I., Sviderskaya, I. v, Babushkina, E.A., Popkova, M.I., Vaganov, E.A., Shishov, V.V., 2019. How can the parameterization of a process-based model help us understand real tree-ring growth. Trees Struct. Funct. 33, 345–357. https://doi.org/10.1007/S00468-018-1780-2.

Vaganov, E.A., Hughes, M.K., Shashkin, A.V., 2006. Growth Dynamics of Tree Rings: Images of Past and Future Environments. Springer, New York.

Valeriano, C., 2017. Plasticidad del Pinus halepensis Mill. frente al cambio climático. Trabajo final del Máster de Ecología, Gestión y Restauración del Medio Natural. Barcelona: Universidad de Barcelona.

Valeriano, C., Gazol, A., Colangelo, M., Camarero, J.J., 2021a. Drought drives growth and mortality rates in three pine species under Mediterranean conditions. Forests 12, 1700. https://doi.org/10.3390/F12121700.

Valeriano, C., Gazol, A., Colangelo, M., González de Andrés, E., Camarero, J.J., 2021b. Modeling climate impacts on tree growth to assess tree vulnerability to drought during forest dieback. Front. Plant Sci. 12, 672855 https://doi.org/10.3389/fpls.2021.672855.

Vieira, J., Rossi, S., Campelo, F., Freitas, H., Nabais, C., 2013. Seasonal and daily cycles of stem radial variation of *Pinus pinaster* in a drought-prone environment. Agric. For. Meteorol. 180, 173–181. https://doi.org/10.1016/J.AGRFORMET.2013.06.009.

Vieira, J., Rossi, S., Campelo, F., Freitas, H., Nabais, C., 2014. Xylogenesis of *Pinus pinaster* under a Mediterranean climate. Ann. For. Sci. 71, 71–80. https://doi.org/10.1007/s13595-013-0341-5.

Vieira, J., Campelo, F., Rossi, S., Carvalho, A., Freitas, H., Nabais, C., 2015. Adjustment capacity of maritime pine cambial activity in drought-prone environments. Plos One 10, e0126223. https://doi.org/10.1371/JOURNAL.PONE.0126223.

Vieira, J., Carvalho, A., Campelo, F., 2020. Tree growth under climate change: evidence from xylogenesis timings and kinetics. Front. Plant Sci. 11, 1–11. https://doi.org/10.3389/fpls.2020.00090.

Wickham, H., 2016. ggplot2: Elegant Graphics for Data Analysis. Springer-Verlag New York.

Wigley, T.M.L., Briffa, K.R., Jones, P.D., 1984. On the average value of correlated time series, with applications in dendroclimatology and hydrometeorology. Journal of Climate and Applied Meteorology 23, 201–213.

Wood, S.N., 2011. Fast stable restricted maximum likelihood and marginal likelihood estimation of semiparametric generalized linear models. J. R. Statist. Soc. B 73, 3–36.

Wood, S.N., 2017. Generalized Additive Models: An Introduction with R. CRC; Boca Raton, USA.

Yang, B., He, M., Shishov, V., Tychkov, I., Vaganov, E., Rossi, S., Ljungqvist, F.C., Bräuning, A., Grießinger, J., 2017. New perspective on spring vegetation phenology and global climate change based on Tibetan Plateau tree-ring data. PNAS 114, 6966–6971. https://doi.org/10.1073/pnas.1616608114.

Zhang, S., Huang, J.G., Rossi, S., Ma, Q., Yu, B., Zhai, L., Luo, D., Guo, X., Fu, S., Zhang, W., 2017. Intra-annual dynamics of xylem growth in *Pinus massoniana* submitted to an experimental nitrogen addition in Central China. Tree Physiol. 37, 1546–1553. https://doi.org/10.1093/TREEPHYS/TPX079.

Zweifel, R., Haeni, M., Buchmann, N., Eugster, W., 2016. Are trees able to grow in periods of stem shrinkage. N. Phytol. 211, 839–849. https://doi.org/10.1111/nph.13995.